



## Research Article

# Virtual Docking Screening and QSAR Studies to Explore PI3K and mTOR Inhibitors Acting on AKT in Cancers

Ilham kandoussi<sup>1\*</sup>, Oussama Benherrif<sup>1</sup>, Wiame Lakhilili<sup>1</sup>, Jamal Taoufik<sup>2</sup>, Azeddine Ibrahim<sup>1</sup>

<sup>1</sup>Laboratory of Biotechnology (MedBiotech), Faculty of Medicine and Pharmacy, Mohammed V University, Rabat, Morocco

<sup>2</sup>Laboratory of Therapeutic Chemistry, Faculty of Medicine and Pharmacy, Mohammed V University, Rabat, Morocco

\***Corresponding Author:** Ilham Kandoussi, Laboratory of Biotechnology (MedBiotech), Faculty of Medicine and Pharmacy, Mohammed V University, Rabat, Morocco, E-mail: [ilham.kandoussi.facmedecine@gmail.com](mailto:ilham.kandoussi.facmedecine@gmail.com)

**Received:** 20 November 2020; **Accepted:** 11 December 2020; **Published:** 04 January 2021

**Citation:** Ilham kandoussi, Oussama Benherrif, Wiame Lakhilili, Jamal Taoufik, Azeddine Ibrahim. Virtual Docking Screening and QSAR Studies to Explore PI3K and mTOR Inhibitors Acting on AKT in Cancers. Journal of Cancer Science and Clinical Therapeutics 5 (2021): 036-048.

### Abstract

The PI3K / AKT / mTOR pathway is an important regulator of a wide range of cellular processes including survival, proliferation, growth, metabolism, angiogenesis and metastasis. PI3K induces translocation of Ser / Thr Akt kinase, Akt is activated by PDK1 and mTOR2-dependent phosphorylations. Aberrant activation of the PI3K / AKT / mTOR pathway is frequently observed in many human malignancies and the combination of compounds simultaneously targeting different related molecules in the PI3K / AKT / mTOR pathway leads to synergistic activity. To explore the common AKT / mTOR and AKT / PI3K competitor ATP inhibitors we performed a 2D AKT-SAR model to predict the bioactivity of PI3K and mTOR

inhibitors on AKT, the interaction of the best inhibitors was evaluated by docking analysis and compared to that of GSK690693 and Ipatasertib. An AKT-SAR model with a correlation coefficient (R<sup>2</sup>) of 0.85212 and an RMSE of 0.09266 was obtained, which was validated and evaluated by a cross-validation method LOO, the most predicted inhibitors of PI3K and mTOR respectively PIC50 activities between [9.30 - 8.54], and [9.79 - 8.91]. After docking and several comparisons, inhibitors with better predictions showed better affinity and interaction with AKT compared to GSK690693 and Ipatasertib. We therefore found that 8 PI3K inhibitors and 11 mTOR inhibitors met the Lipinski and Veber criteria and could be future drugs.

**Keywords:** QSAR; Virtual screening; PI3K/AKT/mTOR; Docking; Dual ATP inhibitors

**Abbreviations:** PI3K- Phosphoinositide 3-Kinase; mTOR- Mammalian Target of Rapamycin; QSAR- Quantitative Structure-Activity Relationship; Ser- Serine; Thr- Threonine; LOO- Leave-one-out; PSA- Polar Surface Area; PLS- Partial Least Square

## 1. Background

The PI3K / AKT / mTOR pathway is hyperactivated or altered in many types of cancer and regulates a wide range of cellular processes, including survival, proliferation, growth, metabolism, angiogenesis, and metastasis. It is regulated by upstream signaling proteins and regulates many downstream effectors by collaborating with various compensatory signaling pathways [1]. There are three AKT isoforms (AKT1, AKT2 and AKT3), which, in general, are widely expressed. AKT is activated by a dual regulatory mechanism that requires both translocation to the plasma membrane and phosphorylation at Thr308 and Ser473 [2, 3]. The generation of PIP3 after PI3K activation recruits AKT by direct interaction with its PH domain. At the membrane level, another PH domain-containing serine / threonine kinase, called 3-phosphoinositide-dependent protein kinase 1 (PDK1), phosphorylates AKT on Thr308 [4]. Phosphorylation of Thr308 is necessary and sufficient for activation of AKT [5]. Studies have shown that overexpression of phosphorylated AKT (p-AKT) is associated with a poor prognosis for a number of solid tumors [6, 7] and some haematological malignancies [8, 9].

Various activating mutations in oncogenes, are found in various malignant tumors in almost every limb of the pathway. Substantial advances in the discovery of PI3K /

AKT / mTOR alterations and their roles in tumorigenesis have led to the development of new targeted molecules with potential for the development of effective anticancer treatment [10]. Inhibition of the PI3K / AKT / mTOR pathway increases antitumor activity [5]. Preclinical data has shown that the combination of compounds simultaneously targeting different molecules of the PI3K / AKT / mTOR pathway leads to synergistic activity [10]. We provide in this study an in silico strategy for the exploration of PI3K AND mTOR inhibitors acting on AKT and therefore competitive dual inhibitors of ATP AKT / PI3K and AKT / mTOR. The marked interest in the development of new AKT / PI3K and AKT / mTOR inhibitors as potential agents for the treatment of cancer prompted us to explore the possibility of developing these inhibitors on the basis of a QSAR / AKT model in order to predict the bioactivity of PI3K and mTOR inhibitors on AKT. The interaction of the best will be evaluated by docking analysis.

## 2. Methodology

### 2.1 Dataset generation

Active inhibitors against AKT were extracted from BINDING DATABASE (<https://www.bindingdb.org>), their IC50 (molecule concentration leading to 50% inhibition) was transformed into logarithmic scale pIC50. 200 compounds with pIC50 greater than 8 were chosen for the present QSAR study. Also, mTOR and PI3K inhibitors with pIC50 greater than 8 have been selected in order to predict their activity against AKT using the AKT-QSAR model and explore their dual activity.

### 2.2 QSAR model generation

184 2D descriptors available on the MOE 2008.10 (obtained from Chemical Computing Group (CCP); Monreal, QC, Canada) [11] were calculated for the 200

compounds. Invariant and insignificant descriptors were initially eliminated; then the QSAR contingency descriptor selection and intercorrelation matrices between descriptor pairs were used to extract the 49 most relevant molecular descriptors which were employed for the distance calculation of each database entry. All 200 selected compounds were distributed randomly in training set with 140 compounds (70% of the data) and test set consisting of 60 compounds (30% of the data). Partial least squares (PLS) analysis based on the leave-one-out (LOO) method was used to correlate molecular descriptors with PIC50 values.

### 2.3 QSAR model validation

The internal validation procedure evaluates the relative predictive performance of the QSAR model, on the one hand by the correlation coefficient ( $R^2$ ) used to measure the correlation between the experimental pIC50 and predicted interest values in order to observe the variability between the variables in the set test, and secondly by the Root Mean Square Error (RMSE) a parameter used to evaluate the relative error of the QSAR model. The model is also tested by cross-validation using the LOO (leave-one-out) method and the computation of the correlation coefficient ( $R^2$ ) and mean squared error [RMSE], Z-Score \$ Z-SCORE and \$ XZ-SCORE are used to detect the outliers. External validation consists of evaluating the activities of the predictions and calculating the numerical parameters using the model.

### 2.4 Activity prediction

The QSAR-AKT model constructed and validated was used to predict the activity of two groups of PI3K and mTOR inhibitors against AKT, A first one is PI3K inhibitors and second one mTOR inhibitors. These inhibitors extracted from the Binding database

(<https://www.bindingdb.org/bind/index.jsp>) have a pIC50 greater than 8 with 477 and 1008 inhibitors for PI3K and mTOR respectively. After calculating the predicted activity, the 40 inhibitors with the best predictions in each group were chosen for docking into AKT to explore their dual activity.

### 2.5 Molecular docking

The 3D coordinates of the mTOR inhibitors as well as the PI3K that showed the best predicted activity on QSAR-AKT model have been generate from 2D. 3MVH (PDB ID) is the AKT crystallized structure recovered from the PDB database for the docking analysis. MGL tools 1.5.6 with AutoGrid4 and AutoDock vina (Scripps) [12] were used for docking studies. The AKT structure was hydrogenated using MGL tools and PyMol was used to visualize the results [13]. In this work we adopted the same docking strategy used by the authors in previous studies [14]. The Grids boxes were generated around the active site of the two three-dimensional structures of the AKT kinase protein using MGL tools 1.5.6. The grids boxes were set to have between 16 and 20Å of edge with coordinates  $x=15.978$ ,  $y=0.806$ ,  $z=29.623$  the coordinates were determined using the potential substrate binding residues as centroids (in the hinge region and the activation loop) [15].

GSK690693 and Ipatasertib, known AKT inhibitors were also docked into AKT and were used as control to evaluate docking results. Their 3D structure was extracted from Pubchem. GSK690393 is a pan-AKT ATP selective inhibitor for AKT kinases [16]. Its potent pharmacodynamic and antitumor activity has been demonstrated in several human tumor cell lines and xenografts [17], growth inhibition and apoptosis in acute lymphoblastic leukemia cell lines [18]. Ipatasertib is a

small molecule inhibitor of AKT, highly competitive orally administered. In cell line and xenograft models, Ipatasertib has been shown to be active in a wide range of cancer types, including breast, ovarian, colorectal and lung cancers [19].

### 3. Results

#### 3.1 QSAR analysis

The AKT-QSAR model was built on the basis of 49 molecular descriptors. After the 200 molecules QSAR regression analysis, a PI3K-SAR model with a correlation coefficient (R<sup>2</sup>) of 0.85212 and a RMSE of 0.09266 was obtained, which was validated and evaluated by a cross-validation method LOO. The predictive performance of this model was represented by cross-validated RMSE with 0.53855 and R<sup>2</sup> with cross-validation of 0.68474. Figure 1 shows a plot of experimental and predicted inhibitory potency in pIC<sub>50</sub> values of the training and test set compounds showing a comparable and similar distribution between the two groups. No outliers were observed in the test set data, and all compounds were well-predicted with a

residual value less than one log unit.

#### 3.2 Virtual screening

The AKT-QSAR model developed and validated was used to predict the activity of PI3K and mTOR inhibitors against PI3K. After calculating the predicted activity, the 40 inhibitors presenting the best predictions in each group are chosen to perform their docking into AKT. The best predicted PI3K and mTOR inhibitors present respectively pIC<sub>50</sub> activities between [8.54-9.30], and [8.9-9.79].

#### 3.3 Molecular docking studies

The docking scores (affinity) of the docked the PI3K and mTOR inhibitors in the catalytic site of AKT were set between -7.9 and -11.9 kcal/mol for the PI3K inhibitors group and between -7.8 and -11.9 kcal/mol for the mTOR inhibitors group; GSK690693 and Ipatasertib (AKT reference inhibitors) presented respective scores of -8.1 and -8.6 kcal/mol as reported on Table 1 and 2.

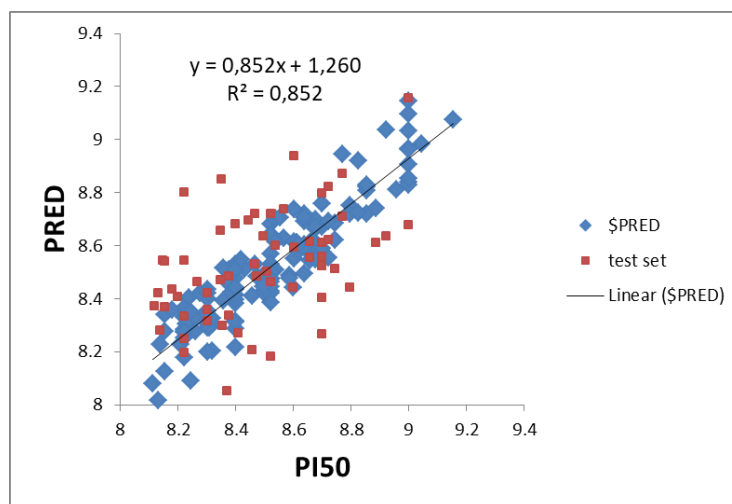


**Figure 1:** Relationship between observed and predicted data from QSAR-AKT model. The compounds of training set are in red and those of test set are in blue. Abbreviations: Pred, Predict; QSAR, quantitative structure-activity relationship.

BindingDB Reactant_set_id	pIC50	Weight	\$PRED	Number of H bonds	Active site residues And Bonds length in Å	Affinity- kcal/mol
235143	8.669	428.423	8.620	5	3.2- 3.4 D292/3.1 L156 / 3.1 E228 / 2.8 A230	9.6
241313	8.316	484.950	8.651	2	3.3 L295 / 3.3 G292	9.5
50225680	9.031	502.578	8.817	4	3.2 K179 / 3.0 T195 / 3.2 - 3.5 E191	10.4
50225682	8.853	474.569	8.622	3	3.2 D292 / 3.1 G294 / 3.0 L295	9.1
50342300	9.638	515.951	8.654	2	3.3 D292 / 3.4 D438	10.8
50342301	8.769	495.534	8.549	2	3.3 D292 / 3.4 D438	11.5
50342304	8.677	511.532	8.583	2	3.1 K158 / 3.6 T195	11.3
50348643	8.187	632.740	8.796	4	3.2 - 3.4 E234 / 3.0 K179 / 3.2 G294	11.4
50409987	8.346	424.44	8.875	6	3.3 E234 / 3.0 D292 / 3.2 - 3.4 T291 / 3.2 E278 / 3.2 K158	8.9
50554599	8.522	515.578	8.562	3	3.4 - 3.0 K158 / 3.3 K179	9.0
50554601	8.221	543.632	8.542	3	2.9 T195 / 3.1 - 3.4 T291	9.9
50554602	9	558.646	8.599	3	3.4 - 3.1 T291 / 2.8 T195	9.8
50554603	8.167	592.664	8.877	4	3.4 K279 / 3.2 K180 / 3.4 - 3.2 T291	10.2
50554604	8.494	613.726	8.652	1	3.1 K179	9.1
50554605	8.619	572.674	8.587	3	3.5 - 3.2 T291 / 2.8 T195	10.3
50570130	9	400.389	8.677	4	3.4 K163 / 3.2 D292 / 3.3 K179 / 2.8 E191	10.1
50570911	8.698	457.493	8.953	4	3.5 K276 / 3.4 D274 / 3.2 E234 / 2.8 T195	8.3
50570918	8.154	527.633	8.798	3	3.1 K179 / 3.4 G159 / 3.2 E234	10.1
50570924	8.744	556.670	8.651	3	3.4 - 3.2 T291 / 2.9 T195	9.6
50570926	9.096	554.654	8.688	2	3.4 G294 / 3.3 K179	7.9
50581032	9.301	534.575	9.038	3	3.4 G294 / 3.3 E198 / 2.9 T195	10.5
50581034	9.397	489.506	8.929	4	3.2 E234 / 2.7 D292 / 3.0 K179 / 3.3 T195	9.9
50581036	9	552.565	9.275	3	3.3 E234 / 3.3 K276 / 2.9 K179	11.9
50581038	9.698	646.703	8.909	2	3.3 K179 / 2.9 E234	10.2
50581040	9.698	659.747	8.961	2	3.4 H194 3.4 D 439	8.9
50581042	9.522	661.763	8.995	1	3.4 H294	9.4
50581044	9.301	664.693	9.145	3	3.1 - 3.4 D292/ 3.3 E 234	10.1

50581046	9.698	679.752	9.233	2	3.1 K179 / 3.3 V164	9.3
50581053	9.397	471.517	8.691	3	3.4 K179 / 2.8 D292 / 3.3 E234	10.1
50602366	8.769	386.414	8.634	2	3.1 - 3.5 T291	9.5
50632672	9.221	349.354	8.609	4	3.2 E234 / 2.8 Y437 / 2.6 L156 / 3.3 D439	10.1
50703938	9.154	483.600	8.561	3	3.5 G311 / 3.2 T195 / 3.5 L156	9.1
50703939	8.677	497.627	8.626	2	3.2 E228 / 3.2 E234	9.8
50703940	9	511.655	8.641	3	2.9 E234 / 3.4 G311 / 2.9 T195	9.6
50881593	9.096	512.573	9.309	5	3.4 - 3.3 D292 / 3.3 N279 / 3.4 E278 / 2.8 L156	9.8
50927439	8.130	416.445	8.852	2	3.5 N279 / 3.5 L156	10.7
51043991	8.167	573.721	8.554	3	3.4 H194 / 3.3 E191 / 3.0 T195	11.0
51065310	8.397	460.541	8.955	2	3.3 K179 / 3.5 D439	9.1
51065317	8.346	419.488	8.600	3	3.4 - 3.1 K179 / 3.1 D439	9.8
51065318	9.148	389.462	8.583	1	3.4 - 3.1 K179 / 3.1 D439	9.7
GSK690693	8.698	425.5	*****	5	1.8 G311 / 3.5 K179 / 3.0 T195 / 2.2 E191 / 2.9 G159	8.1
IPATASERTIB	8.301	458	*****	1	2.8 E234	8.5

The docking (affinity) scores of PI3K inhibitors in the catalytic site of AKT were set between -7.9 and -11.9 kcal / mol. GSK690693 and Ipatasertib (AKT reference inhibitors) showed scores of -8.1 and -8.6 kcal / mol

**Table 1:** Docked interaction analysis of PI3K inhibitors screened into AKT.

BindingDB Reactant_set_id	PIC50	Weight	\$PRED	Number of H bonds	Active site residues And Bonds length in Å	Affinity - kcal/mol
240612	8.866	485.497	8.913	1	3.4 E234	10.1
240614	8.756	499.524	8.980	0	0	11.1
240621	8.653	515.979	8.934	2	3.5 G162 / 3.2 K276	10.3
240722	9.091	495.561	8.933	2	3.2 K179 / 3.4 N279	9.2
240723	8.835	496.549	8.924	1	3.2 D439	10.2
240724	8.787	509.588	9.000	1	3.2 K179	8.9
240755	9.677	543.578	8.921	3	3.3 K276 / 3.1- 3.1 T311	10.6
240758	9.309	557.604	8.983	1	3.0 K179	11.3
240765	9.346	574.06	8.938	1	3.2 K179	11.4
270328	8.193	462.468	8.916	4	3.3 - 3.0 K179 / 3.2 - 3.1 G294	10.1

270339	9.292	493.860	9.106	4	3.4 - 2.9 K179 / 3.4 - 3.3 G294	10.7
270346	9.060	477.405	9.124	4	3.3 - 2.9 K179/3.1 - 3.2 G294	9.9
270348	9.292	460.403	9.005	4	3.4- 2.9 K129/ 3.1 - 3.2 G294	9.7
270352	9.292	459.415	8.984	3	2.9 K179/ 3.2 - 3.2 G294	9.3
270356	8.886	459.415	8.957	1	3.2 K179	11.0
270358	8.698	476.858	8.973	3	3.6K276 / 3.2 K179 / 3.5 T291	10.6
270368	8.568	472.44	8.939	2	3.3 G294 /3.0 K179	10.7
270370	9.102	474.431	9.089	3	3.3 - 2.9 G294 / 3.1 K179	11.1
270372	8.602	474.431	9.006	3	3.4 K276 / 3.2 K158 / 2.9 T159	10.9
270379	8.187	474.431	9.066	4	3.3 - 3.2 G294 / 2.9 - 3.3 K179	11.5
270380	8.346	457.424	8.945	5	3.3 - 3.0 / 3.1 - 3.5 K179 / 3.4 E234	10.1
270383	8.455	460.403	9.005	4	3.4 - 2.9 K179 / 3.1 - 3.1 G294	9.8
270386	8.200	476.402	9.171	5	3.1 E234 / 2.9 - 3.5 K179 /3.2 - 3.2 G294	10.8
50570952	8.522	457.493	8.953	4	2.8 T195 / 3.4 D274 / 3.5 K276 / 3.2 E234	8.6
50581033	8.283	534.575	9.038	3	3.5 T195 / 3.5 K179 / 2.9 E234	10.3
50581035	8.619	489.506	8.929	4	3.3 T195 / 2.7 D192 / 3.1 K179 / 2.7 D291 / 3.1 E234	9.9
50581037	8.823	552.565	9.275	3	3.4 K276 / 2.9 K179 / 3.3 E234	11.9
50581041	8.420	659.747	8.961	1	3.4 H194	8.4
50581043	8.958	661.763	8.995	3	3.2 E234 / 3.2 G294 / 3.4 T195	8.1
50581045	8.602	664.693	9.145	3	3.1 - 3.5 D292 / 3.3 E234	10.2
50581047	9.522	679.752	9.233	2	2.8 D292 / 3.4 K158	7.8
50966358	8.522	388.394	9.023	4	3.3 - 3.4 - 3.3 T291 / 3.3 E278	8.0
50966360	8.301	387.410	9.092	3	3.3 D292 / 3.5 T291 / 3.3 E234	9.9
50966362	8.522	399.422	9.084	2	3.3 K158 / 3.0 T195	10.0
50966363	8.698	385.394	9.000	2	3.3 E234 / 3.4 D294	9.3
50966364	8.397	398.433	8.917	1	3.4 N279	10.1
50966368	8.522	398.433	8.917	3	3.0 D439 / 3.3 D292 / 3.5 T291	10.2
50966398	8.522	415.420	9.793	3	3.4 - 3.2 D292 / 3.3 T195	8.7
50966403	8.221	385.394	9.711	2	3.1 K179 / 3.3 D292	9.1
50966404	8.522	349.358	9.310	3	3.5 - 3.5 D292 / 3.3 E234	8.5

GSK 690693	8.698	425.5g	*****	5	1.8 G311 / 3.5 K179 / 3.0 T195 / 2.2 E191 / 2.9 G159	8.1
IPATASERTIB	8.301	458	*****	1	2.0 G159	8.5

The docking (affinity) scores of mTOR inhibitors in the catalytic site of AKT were set between -7.8 and -11.9 kcal / mol. GSK690693 and Ipatasertib (AKT reference inhibitors) showed scores of -8.1 and -8.6 kcal / mol

**Table 2:** Docked interaction analysis of mTOR inhibitors screened into AKT.

#### 4. Discussion

Almost all intervenanants of the pathway may be affected by various mutations inducing malignant tumors. The discovery of PI3K / AKT / mTOR alterations and their role in tumorigenesis have allowed the development of new molecules with inhibitory activity and continuous development for an anticancer treatment. In order to explore new AKT/PI3K and AKT/mTOR common inhibitors, a 2D-QSAR model for AKT was constructed to predict the activity of one group of PI3K inhibitors and one of mTOR, then do the docking for those who presented the best prediction (the top 40 in each group) whose results were compared with that of GSK 690693 and Ipatasertib. The AKT inhibitors that were used in the construction of the QSAR model and those of PI3K and mTOR whose activity for AKT was predicted were extracted from Binding Database and selected according to their bioactivity IC50, the model was realized by the PLS method by the MOE software. AKT and mTOR inhibitors docking score compared to GSK 690693 and Ipatasertib score show that the PI3K inhibitors and those of mTOR respectively have an affinity between -7.9 and -11.9 kcal/mol and -7.8 and -11.9 kcal/mol while GSK 690693 and Ipatasertib only -8.1 and -8.5 kcal/mol, respectively, therefore, 39 PI3K inhibitors and 37 mTOR inhibitors show higher affinity than that of GSK 690693 and 38 PI3K inhibitors and 35 mTOR inhibitors show higher affinity than that of Ipatasertib. Thus, the affinity of Ipatasertib is

more effective than that of GSK 690693 the opposite for the interactions. Visualization of these interactions showed that the different compounds adapt to the ATP binding site forming hydrogen bonds, the best PI3K-inhibitor establishes 6 bonds Hydrogens with AKT, that of mTOR establishes 5 bonds against the GSK 690693 and Ipatasertib have respectively 5 and only 1 connection. The important score of the affinity of some inhibitors despite the low number of hydrogen bonds can be explained by the hydrophobic interactions and that of Van Der Waal. Thus, the AKT affinity of most of the PI3K and mTOR inhibitors studied is more effective than that of GSK 690693 and Ipatasertib and the majority interaction is more effective than that of Ipatasertib. A phase 1 clinical study demonstrated robust inhibition of the AKT pathway by Ipatasertib at clinically feasible doses [20] and other studies of various types of tumors, including breast cancer, have shown an acceptable safety profile but characterized by gastrointestinal effects, asthenia or fatigue and rash [21].

A double comparison of the inhibitors studied with respect to GSK690693 which, given the affinity and the number of hydrogen bonds greater than 4 mediated by AKT, showed that 10 PI3K inhibitors (Table 3) and 11 mTOR inhibitors (Table 4) all have better results than GSK690693, but taking into account Lipinski's rules (no more than 5 hydrogen bond donors, no more than 10 hydrogen bond



acceptors, an octanol-water partition coefficient no greater than 5,5) and those of Veber determining the good bioavailability (PSA (Polar surface)  $\leq 140 \text{ \AA}^2$  (absolute polarity measurement), rotary links  $\leq 10$  (measure of flexibility, we found that 7 PI3K inhibitors (Table 5) of which 50409987 the most relevant (6 hydrogen bonds and an affinity -8,9/ mol) and 10 mTOR inhibitors (Table 6), of which the 270386 is the most relevant (5 hydrogen bonds and an affinity of -10.8 kcal / mol) corresponded to all criteria and could be future drugs (Figure 2), but knowing

that GSK690693 has demonstrated broad in vitro activity, and that in vivo results against solid tumors demonstrate that GSK690693 has only modest antitumor activity and thus the use of GSK690693 as a unique agent in the treatment Malignant tumors in children will probably have limited value without further optimization [22], according to our study, inhibitors with an affinity and an interaction as important as GSK690693, which can act as inhibitors of AKT in addition to their action. On either the PI3K or the mTOR would be important.

BindingDB Reactant_set_id	\$PRED	Weight	HD	AFFINIY	b_rotN	a_acc	a_don	SlogP	TPSA
50409987	8,875	424.44	6	8,9	5	6	3	2,550	136,89
235143	8,620	428.423	5	9,6	6	6	2	0,830	146,55
50881593	9,309	512.573	5	9,8	8	7	5	3,414	127,51
50225680	8,817	502.578	4	10,4	6	7	1	3,175	116,12
50348643	8,796	632.74	4	11,4	13	6	3	5,707	135,2
50554603	8,877	592.664	4	10,2	12	8	3	4,022	152,08
50570130	8,677	400.389	4	10,1	3	5	3	4,265	104,67
50570911	8,953	457.493	4	8,3	8	6	2	3,439	114,27
50581034	8,929	489.506	4	9,9	6	4	3	5,059	110,27
50632672	8,609	349.354	4	10,1	3	6	4	2,255	135

PI3K inhibitors with better affinity and number of hydrogen bonds than GSK 690693

**Table 3:** Comparison of PI3K inhibitors studied to GSK 690693.

BindingDB Reactant_set_id	\$PRED	Weight	HB	AFFINITY	b_rotN	a_acc	a_don	SlogP	TPSA
270380	8.945	457.424	5	10.1	4	5	1	4.124	124.66
270386	9.171	476.402	5	10.8	4	6	1	3.658	137.55
270328	8.916	462.468	4	10.1	4	7	2	4.042	114.18
270339	9.106	493.860	4	10.7	4	6	2	5.070	101.29
270346	9.124	477.405	4	9.9	4	6	2	4.555	101.29
270348	9.005	460.403	4	9.7	4	7	2	3.811	114.18
270379	9.066	474.431	4	11.5	4	7	2	4.120	114.18

270383	9.005	460.403	4	9.8	4	7	2	3.811	114.18
50570952	8.953	457.493	4	8.6	8	6	2	3.439	114.27
50581035	8.929	489.506	4	9.9	6	4	3	5.059	110.27
50966358	9.023	388.394	4	8.0	4	7	4	2.413	149.25

mTOR inhibitors with better affinity and number of hydrogen bonds than GSK 690693

**Table 4:** Comparison of mTOR inhibitors studied to GSK 690693.

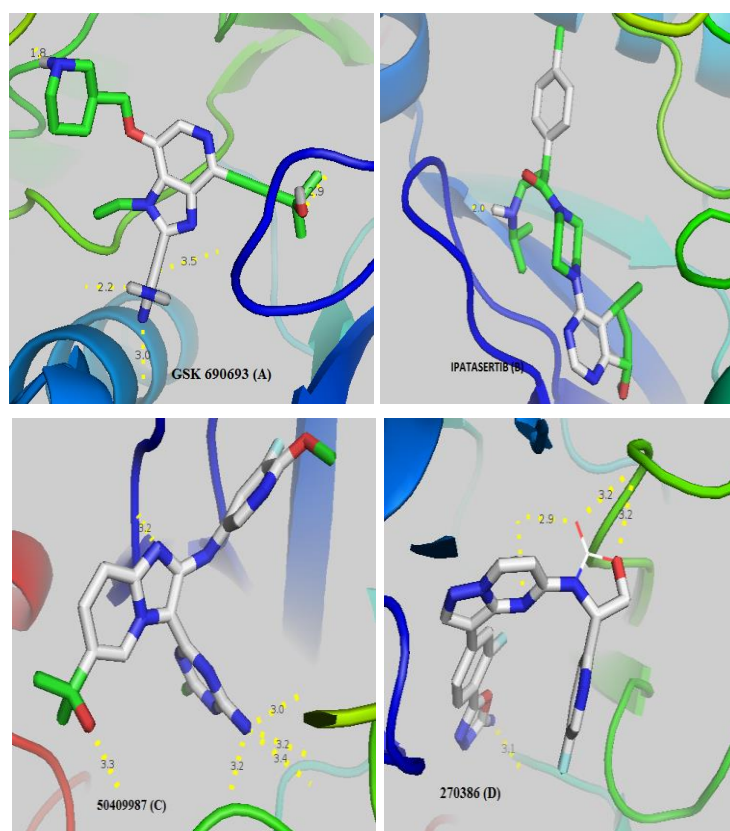
BindingDB Reactant_set_id	Name
5E+07	2-[3-(4-amino-6-methyl-1,3,5-triazin-2-yl)-2-[(5-fluoro-6-methoxypyridin-3-yl)amino]imidazo[1,2-a]pyridin-6-yl]propan-2-ol
5E+07	7-(2-(1-(2-(dimethylamino)acetyl)-5-methoxyindolin-6-ylamino)-7H-pyrrolo[2,3-d]pyrimidin-4-ylamino)isoindolin-1-one
5E+07	(2S)-2-hydroxy-1-[3-[4-[2-(5-methyl-2-propan-2-yl-1,2,4-triazol-3-yl)-5,6-dihydroimidazo[1,2-d][1,4]benzoxazepin-9-yl]pyrazol-1-yl]azetid-1-yl]propan-1-one
5E+07	4,6-dihydroxy-2-((5-methoxy-2-(pyridin-3-yl)-1H-indol-3-yl)methylene)benzofuran-3(2H)-one
5E+07	1-[4-[4-morpholin-4-yl-7-(2-oxoethyl)pyrrolo[2,3-d]pyrimidin-2-yl]phenyl]-3-pyridin-4-ylurea
5E+07	1-(2-((7-fluoro-5-methoxy-2-(1,3,5-trimethyl-1H-pyrazol-4-yl)-1H-indol-3-yl)methylene)-3-oxo-2,3-dihydrobenzofuran-5-yl)-3-methylurea
5E+07	5-(1-(4-amino-6-methyl-1,3,5-triazin-2-yl)-1H-benzo[d]imidazol-2-ylamino)benzene-1,3-diol

**Table 5:** PI3K inhibitors meeting Lipinski and Veber criteria.

BindingDB Reactant_set_id	Name
270380	(4S)-3-[3-[4-(5-amino-1,3,4-oxadiazol-2-yl)phenyl]pyrazolo[1,5-a]pyrimidin-5-yl]-4-(4-fluorophenyl)-1,3-oxazolidin-2-one
270386	(4S)-3-[3-[4-(5-amino-1,3,4-oxadiazol-2-yl)-3-fluorophenyl]pyrazolo[1,5-a]pyrimidin-5-yl]-4-(5-fluoropyridin-2-yl)-1,3-oxazolidin-2-one
270328	(4R)-3-[3-[3-fluoro-4-(1H-1,2,4-triazol-5-yl)phenyl]pyrazolo[1,5-a]pyrimidin-5-yl]-4-(4-methyl-1,3-thiazol-2-yl)-1,3-oxazolidin-2-one
270339	(4S)-4-(3-chloro-4-fluorophenyl)-3-[3-[3-fluoro-4-(1H-1,2,4-triazol-5-yl)phenyl]pyrazolo[1,5-a]pyrimidin-5-yl]-1,3-oxazolidin-2-one
270346	(4S)-4-(3,4-difluorophenyl)-3-[3-[3-fluoro-4-(1H-1,2,4-triazol-5-yl)phenyl]pyrazolo[1,5-a]pyrimidin-5-yl]-1,3-oxazolidin-2-one

270348	(4S)-4-(5-fluoropyridin-2-yl)-3-[3-[3-fluoro-4-(1H-1,2,4-triazol-5-yl)phenyl]pyrazolo[1,5-a]pyrimidin-5-yl]-1,3-oxazolidin-2-one
270379	(4S)-4-(3-fluoro-6-methylpyridin-2-yl)-3-[3-[3-fluoro-4-(1H-1,2,4-triazol-5-yl)phenyl]pyrazolo[1,5-a]pyrimidin-5-yl]-1,3-oxazolidin-2-one
270383	(4S)-4-(5-fluoropyridin-2-yl)-3-[3-[3-fluoro-4-(1H-1,2,4-triazol-5-yl)phenyl]pyrazolo[1,5-a]pyrimidin-5-yl]-1,3-oxazolidin-2-one
50570952	1-[4-[4-morpholin-4-yl-7-(2-oxoethyl)pyrrolo[2,3-d]pyrimidin-2-yl]phenyl]-3-pyridin-4-ylurea
50581035	1-[(2E)-2-[[7-fluoro-5-methoxy-2-(1,3,5-trimethylpyrazol-4-yl)-1H-indol-3-yl]methylidene]-3-oxo-1-benzofuran-5-yl]-3-methylurea

**Table 6:** mTOR inhibitors meeting Lipinski and Veber criteria.



GSK690693 (A) and Ipatasertib (B) respectively have 5 and 1 linkages with the catalytic site of AKT whereas 50409987 inhibitor of PI3K (C) and 270386 inhibitor of mTOR (D) respectively have 6 and 5 hydrogen bonds. Notes: red zones: oxygen atom, blue zones, nitrogen atom and green zones, other. The hydrogen bonds are represented by the dashed yellow. The numbers represent the size of the hydrogen bonds established between the ligand and the receptor.

**Figure 2:** Visualization of the different interactions between the compounds and the active site of AKT via the hydrogen bonds.

## 5. Conclusion

The hyperactivation of PI3K / Akt / mTOR in cancer, associated with the crucial role of AKT signaling in tumorigenesis, has led to significant efforts to generate inhibitors to target this pathway. Through the construction of a QSAR-AKT model, we were able to predict potent PI3K and mTOR inhibitor activity on AKT select the best and reveal their interactions with AKT by docking while comparing them to AKT reference inhibitors. Promising results have been obtained. The dual inhibitors AKT / PI3K and AKT / mTOR have been predicted, pending the testing of these compounds directly on the cancer cell lines in our next study.

## References

1. Ersahin T, Tuncbag N, Cetin-Atalay R. The PI3K/AKT/mTOR interactive pathway. *Mol Biosyst* 11 (2015): 1946-1954.
2. Bellacosa A, Chan TO, Ahmed NN, et al. Akt activation by growth factors is a multiple-step process: the role of the PH domain. *Oncogene* 17 (1998): 313-325.
3. Andjelković M, Alessi DR, Meier R, et al. Role of translocation in the activation and function of protein kinase B. *J Biol Chem* 272 (1997): 31515-31524.
4. Vanhaesebroeck B, Alessi DR. The PI3K-PDK1 connection: more than just a road to PKB. *Biochem J* 346 (2000): 561-576.
5. Vivanco I, Sawyers CL. The phosphatidylinositol 3-Kinase-AKT pathway in human cancer. *Nat Rev Cancer* 2 (2002): 489.
6. Schmitz KJ, Otterbach F, Callies R, et al. Prognostic relevance of activated Akt kinase in node-negative breast cancer: a clinicopathological study of 99 cases. *Mod Pathol Off J U S Can Acad Pathol Inc* 17 (2004): 15-21.
7. Dai DL, Martinka M, Li G. Prognostic significance of activated Akt expression in melanoma: a clinicopathologic study of 292 cases. *J Clin Oncol Off J Am Soc Clin Oncol* 23 (2005): 1473-1482.
8. Rudelius M, Pittaluga S, Nishizuka S, et al. Constitutive activation of Akt contributes to the pathogenesis and survival of mantle cell lymphoma. *Blood* 108 (2006): 1668-1676.
9. Min YH, Eom JI, Cheong JW, et al. Constitutive phosphorylation of Akt/PKB protein in acute myeloid leukemia: its significance as a prognostic variable. *Leukemia* 17 (2003): 995-997.
10. Polivka J, Janku F. Molecular targets for cancer therapy in the PI3K/AKT/mTOR pathway. *Pharmacol Ther* 142 (2014): 164-175.
11. Vilar S, Moro GC S. Medicinal Chemistry and the Molecular Operating Environment (MOE): Application of QSAR and Molecular Docking to Drug Discovery [Internet]. *Current Topics in Medicinal Chemistry* (2008).
12. Trott O, Olson AJ. AutoDock Vina: improving the speed and accuracy of docking with a new scoring function, efficient optimization and multithreading. *J Comput Chem* 31 (2010): 455-461.
13. Seeliger D, de Groot BL. Ligand docking and binding site analysis with PyMOL and Autodock/Vina. *J Comput Aided Mol Des* 24 (2010): 417-422.
14. Lakhilili W, Chevé G, Yasri A, et al. Determination and validation of mTOR kinase-domain 3D structure by homology modeling. *OncoTargets Ther* 8 (2015): 1923-1930.

15. Lakhilili W, Yasri A, Ibrahim A. Structure–activity relationships study of mTOR kinase inhibition using QSAR and structure-based drug design approaches. *OncoTargets Ther* 9 (2016): 7345-7353.
16. Heerding DA, Rhodes N, Leber JD, et al. Identification of 4-(2-(4-amino-1,2,5-oxadiazol-3-yl)-1-ethyl-7-[[[(3S)-3-piperidinylmethyl]oxy]-1H-imidazo[4,5-c]pyridin-4-yl]-2-methyl-3-butyn-2-ol (GSK690693), a novel inhibitor of AKT kinase. *J Med Chem* 51 (2008): 5663-5679.
17. Rhodes N, Heerding DA, Duckett DR, et al. Characterization of an Akt kinase inhibitor with potent pharmacodynamic and antitumor activity. *Cancer Res* 68 (2008): 2366-2374.
18. Levy DS, Kahana JA, Kumar R. AKT inhibitor, GSK690693, induces growth inhibition and apoptosis in acute lymphoblastic leukemia cell lines. *Blood* 113 (2009): 1723-1729.
19. Targeting Activated Akt with GDC-0068, a Novel Selective Akt Inhibitor That Is Efficacious in Multiple Tumor Models. *Clinical Cancer Research* (2019).
20. Yan Y, Serra V, Prudkin L, et al. Evaluation and clinical analyses of downstream targets of the Akt inhibitor GDC-0068. *Clin Cancer Res Off J Am Assoc Cancer Res* 19 (2013): 6976-6986.
21. Saura C, Roda D, Roselló S, et al. A First-in-Human Phase I Study of the ATP-Competitive AKT Inhibitor Ipatasertib Demonstrates Robust and Safe Targeting of AKT in Patients with Solid Tumors. *Cancer Discov* 7 (2017): 102-113.
22. Carol H, Morton CL, Gorlick R, et al. Initial Testing (Stage 1) of the Akt Inhibitor GSK690693 by the Pediatric Preclinical Testing Program. *Pediatr Blood Cancer* 55 (2010): 1329-1337.



This article is an open access article distributed under the terms and conditions of the [Creative Commons Attribution \(CC-BY\) license 4.0](https://creativecommons.org/licenses/by/4.0/)